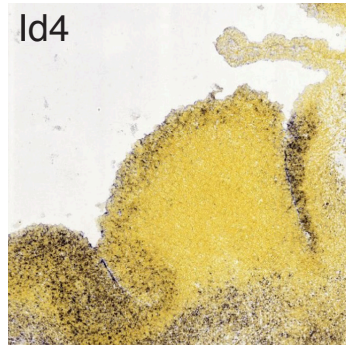
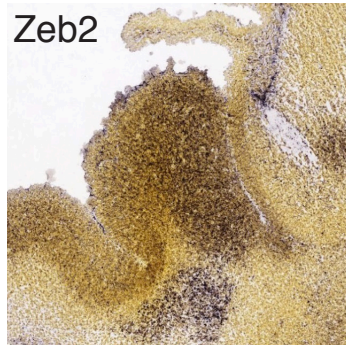
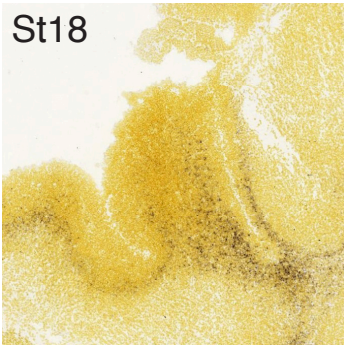
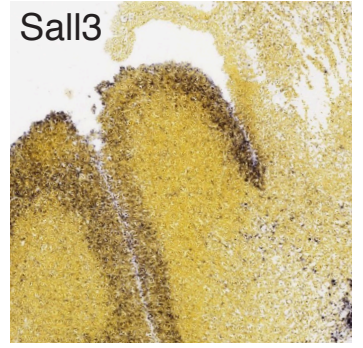
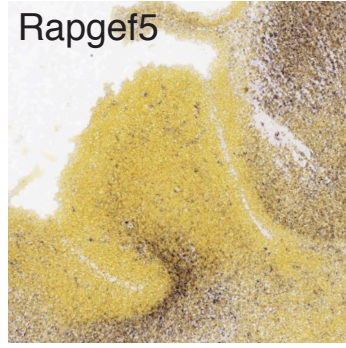
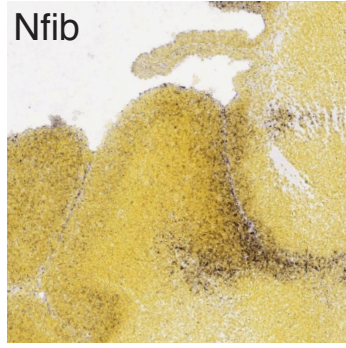
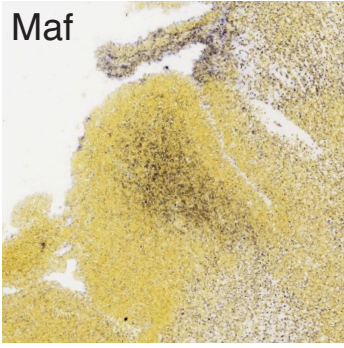
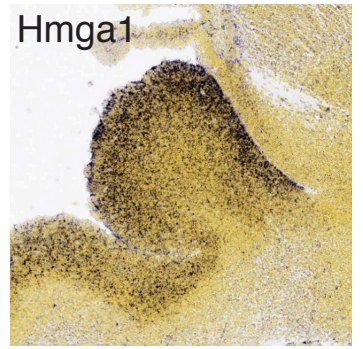
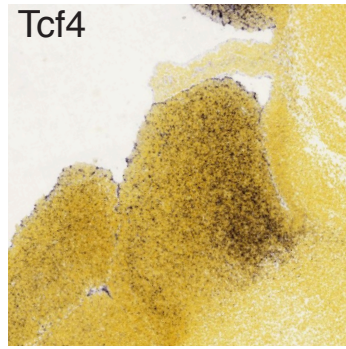
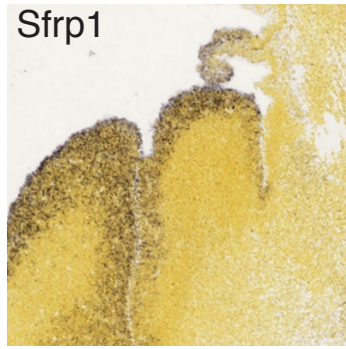
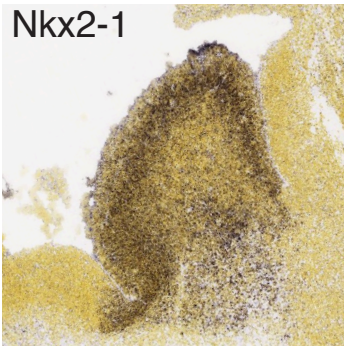


Supplemental Figure 1

**Supplemental Figure 1.** *In situ hybridization patterns for Wnt ligands in the embryonic mouse brain over time. Related to figure 1.*

In situ hybridization for Wnt 7a, Wnt 7b, Wnt 5a and Wnt 3a. Sections in parasagittal plane, see Figure 1B and 4I for orientation of embryonic structures. (Website: ©2013 Allen Institute for Brain Science. Allen Developing Mouse Brain Atlas [Internet]. Available from:

<http://developingmouse.brain-map.org.>)



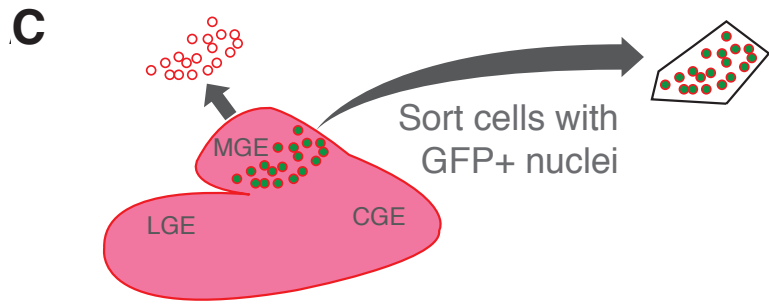
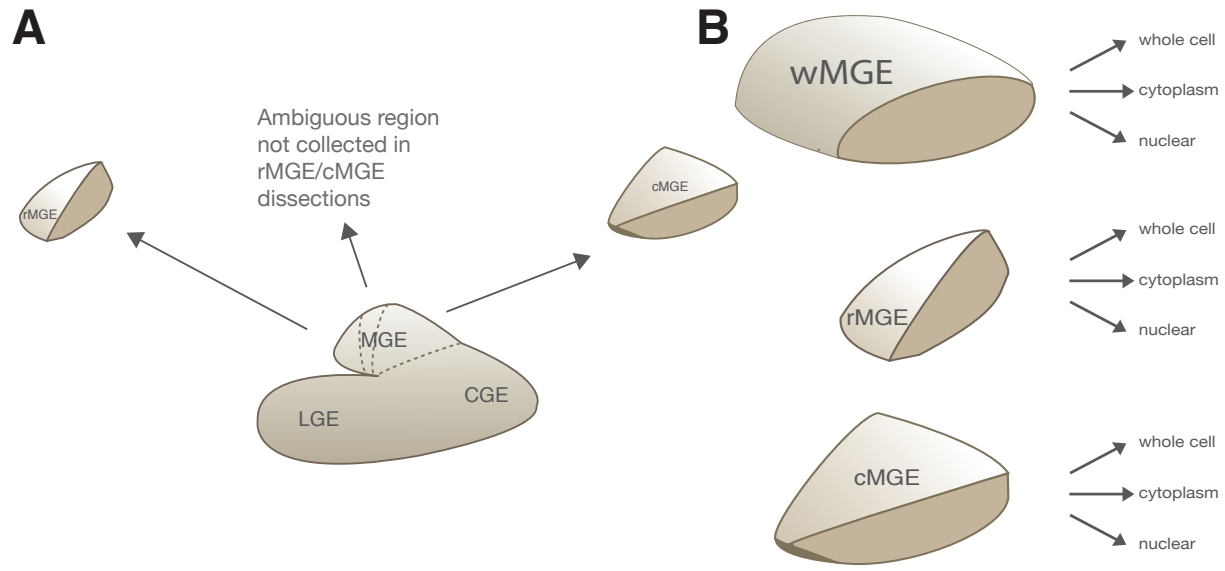
**Supplemental Figure 2**

**Supplemental Figure 2.** *In situ hybridization of genes with caudal/rostral regional expression in the MGE. Related to figure 1.*

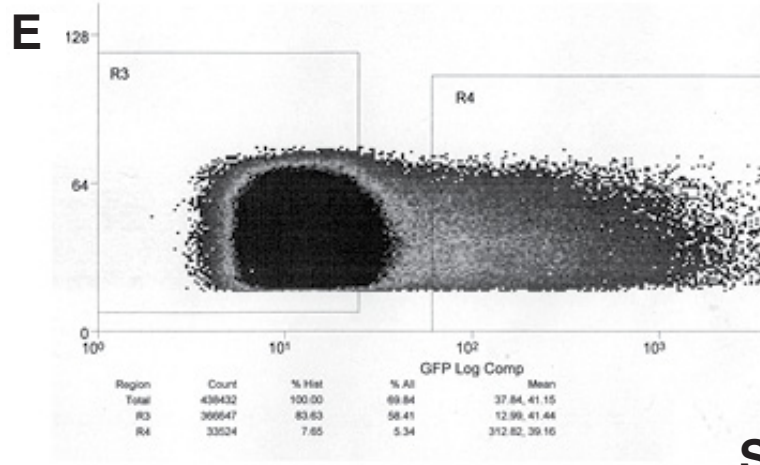
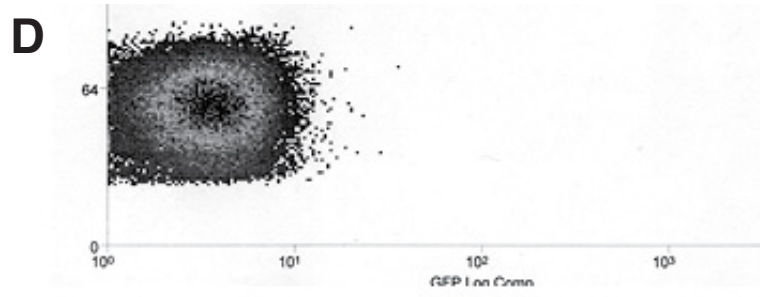
Sections in parasagittal plane, see Figure 1B and 4I for orientation of embryonic structures.

(Website: ©2013 Allen Institute for Brain Science. Allen Developing Mouse Brain Atlas

[Internet]. Available from: <http://developingmouse.brain-map.org>.)



pan-TdTomato; TCF/LEF:H2B-GFP(nuclear)



Supplemental Figure 3

**Supplemental Figure 3.** *Schematic depicting dissection strategy, collection of Wnt-responsive MGE for transplantation and western blot. Related to figures 1, 3, 4.*

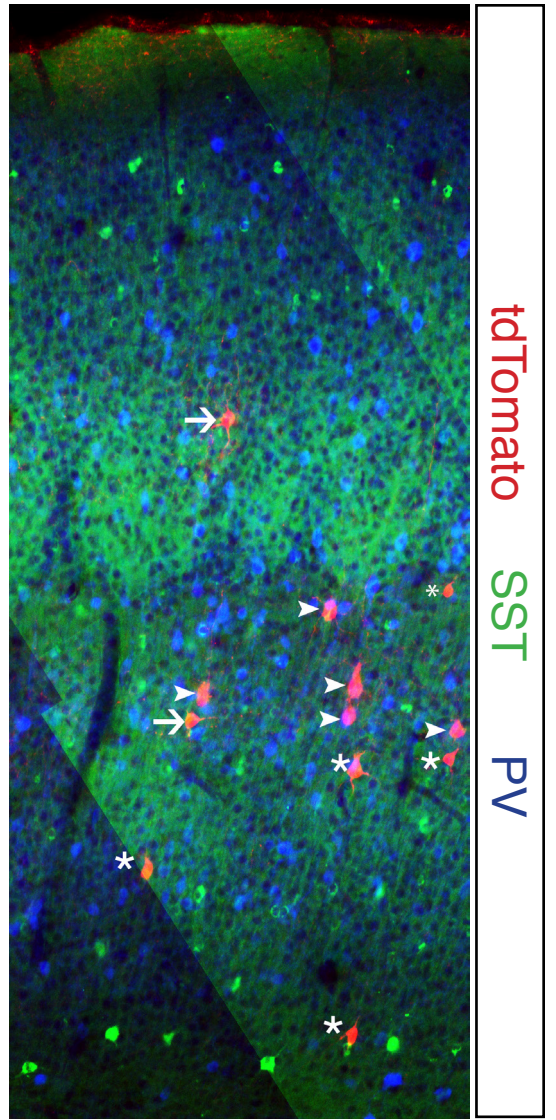
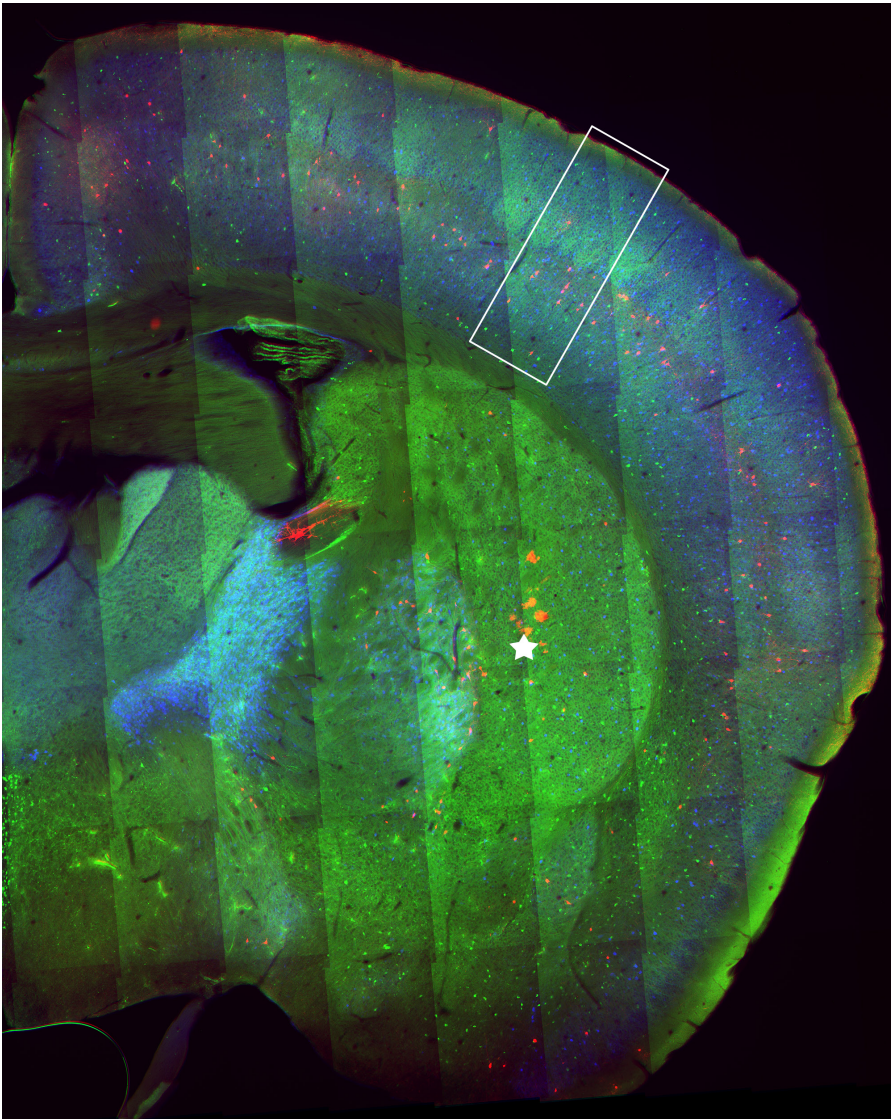
(A) Detailed dissection strategy schematic for experiments described in figure 1. Rostral and Caudal dissections were done independently, such that both rostral and caudal dissections are more conservative and leaves a region of 'ambiguity' that is only collected in wMGE dissections.

(B) Protein collection and fractionation of samples followed dissection as in (A) to perform

experiments described in figure 4. (C) Related to figure 3, whole MGE from e12.5 embryos were single cell dissociated and sorted for nuclear GFP expression of TCF/LEF:H2B-GFP. (D)

Negative control MGE Ai9 pan-expression MGE. (E) TCF/LEF:H2B-GFP; Ai9 pan-expression

MGE. Gated fraction for transplantation is R4, corresponding to 7.7% of the total cell population.



tdTomato SST PV

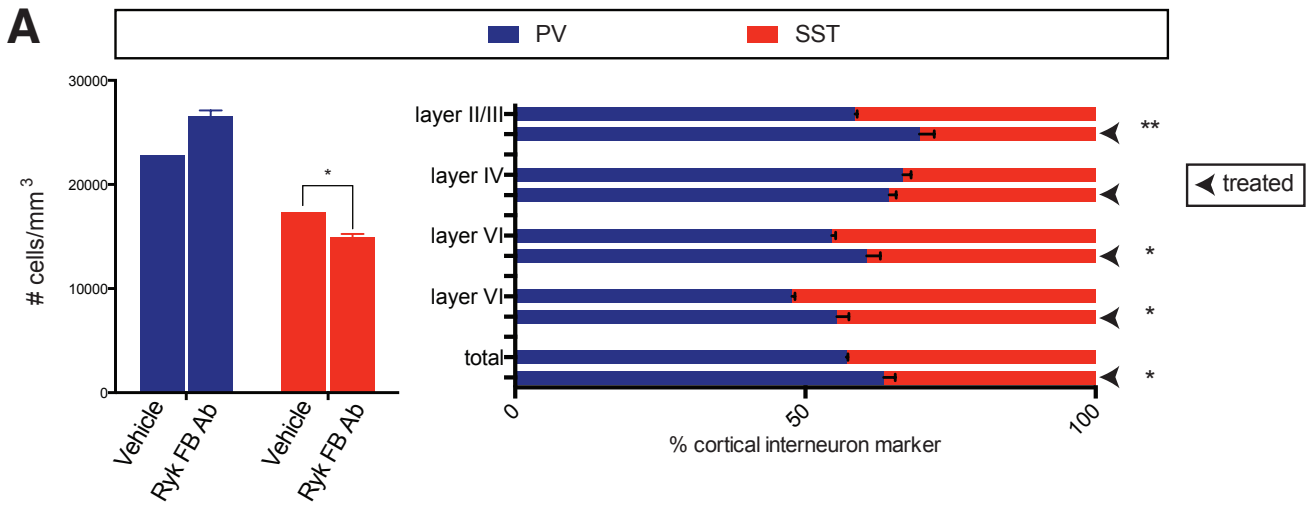
Supplemental Figure 4

**Supplemental Figure 4.** *Postnatal Analysis of Ryk<sup>-/-</sup> MGE transplant. Related to figure 5.*

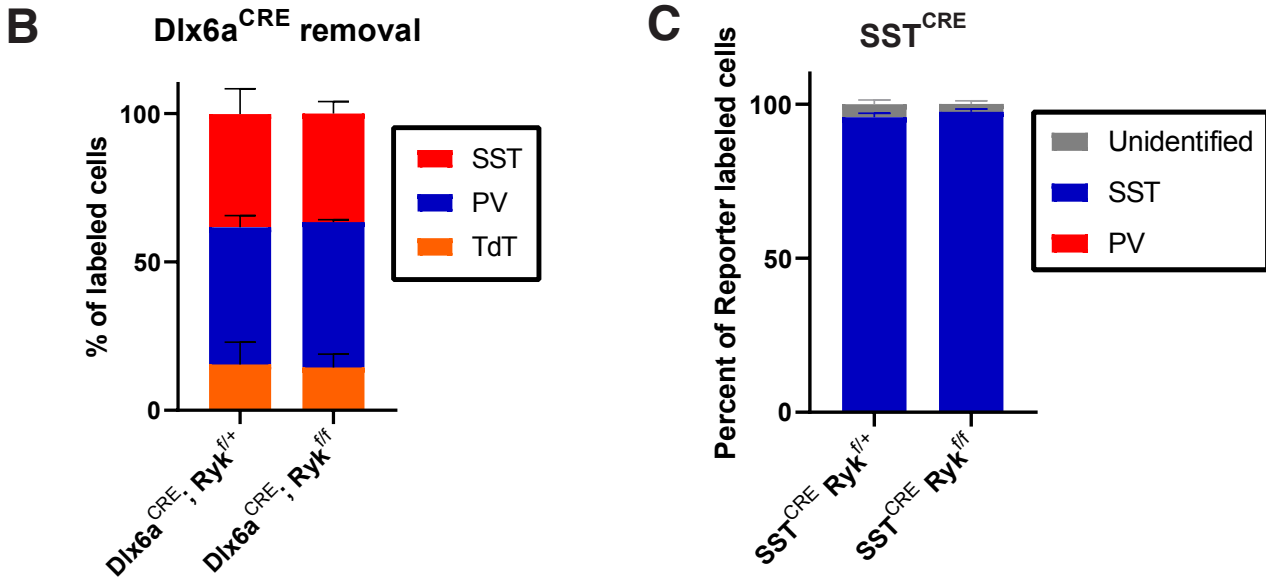
Left, coronal section of P21 mouse brain that received in utero transplantation of tdTomato+ *Ryk<sup>-/-</sup>* MGE. *Ryk<sup>-/-</sup>* cells were capable of robust tangential into host cortex. Star denotes transplant site. Right, higher magnification of boxed region on left. Arrow denotes tdTomato+ (red) cell co-expressing somatostatin (green). Arrowhead denotes tdTomato+ cell co-expressing parvalbumin (blue). Asterisk denotes unidentified tdTomato+ cell.



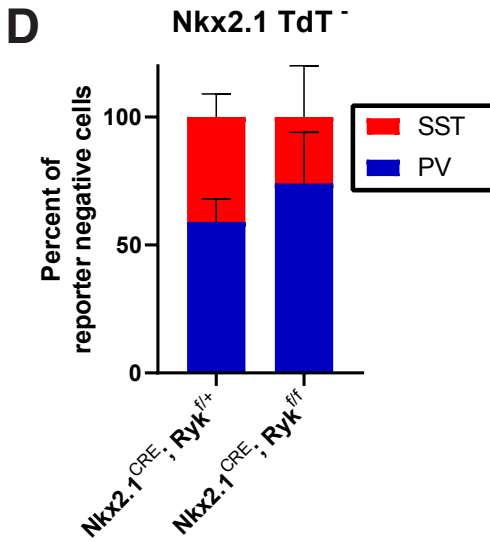
## Ryk Function-Blocking Antibody



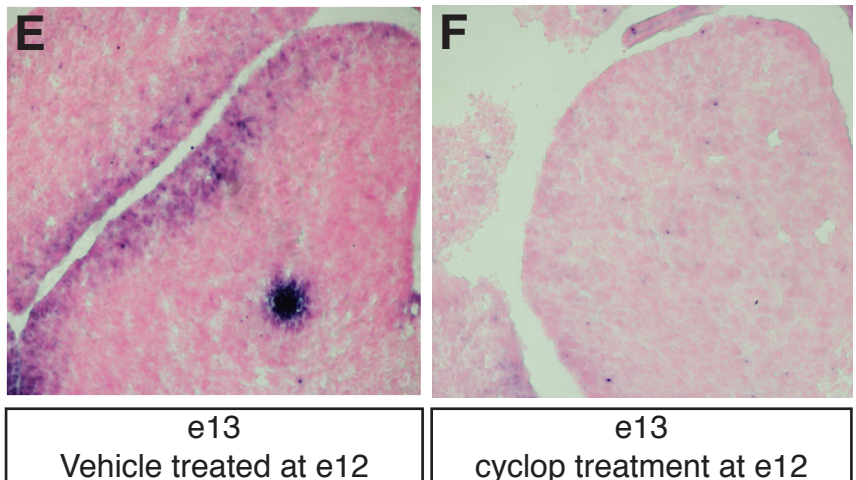
## Post-mitotic Ryk conditional ablation



## Non-cell autonomous effects

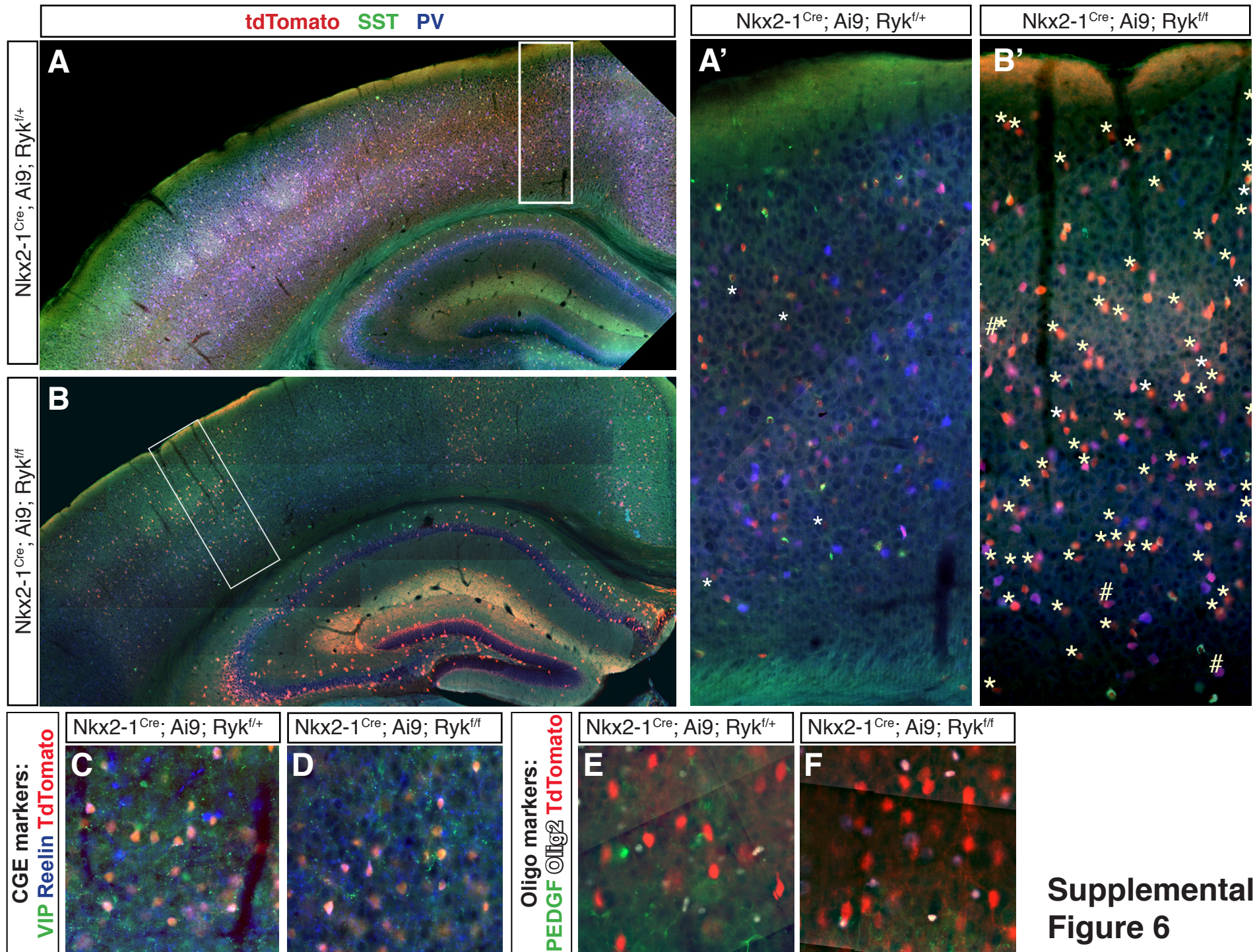


## Gli1 *in situ* hybridization



**Supplemental Figure 5.** *Suppressing Ryk signaling by in utero intraventricular injection of Ryk function-blocking antibody, Post-mitotic Ryk conditional Ryk ablation by  $Dlx6a^{Cre}$  and  $SST^{Cre}$ ; non-cell autonomous analysis of  $Nkx2.1^{Cre}$  Ryk removal, Cyclopamine knockdown of Shh signaling in  $Nkx2.1^{Cre}$  Ryk mutants. Related to figure 5.*

(A) Wildtype mouse e13.5 embryos received intraventricular injection of vehicle or Ryk function-blocking antibody were analyzed at P21. Left, total PV+ and SST+ interneurons by volume. Right, proportion of PV+ and SST+ interneurons by cortical layer. Function blocking antibody (represented in bars denoted by arrows) significantly reduced the numbers of SST+ interneurons in superficial and deep layers of cortex other than layer IV. (B) Quantification of PV and SST cell density in p21 cortex from  $Dlx6a^{Cre}; Ryk^{f/+}$  control and  $Dlx6a^{Cre}; Ryk^{f/f}$  mutants. (C) Quantification of PV and SST cell density in reporter labeled (TdTomato) cells in  $SST^{Cre}; Ryk^{f/+}$  control and  $SST^{Cre} Ryk^{f/f}$  mutant cells. There are no significant differences between the frequency of PV and SST labeled cells following post-mitotic removal of *Ryk*. Furthermore, SST cells with *Ryk* removed post-mitotically retain SST identity and do not adopt a PV+ fate. (D) PV and SST cell density in non-reporter labeled (TdTomato-negative) cells in  $Nkx2.1^{Cre}; Ryk^{f/+}$  control and  $Nkx2.1^{Cre} Ryk^{f/f}$  mutant cortex at p21. Non-reporter labeled cells are non-significantly biased toward a PV fate. (E-F) *In situ* hybridization for *Gli1* in E13.5 wild type embryos treated with vehicle (E) or cyclopamine (F) at e12.5 show a reduction in signal with treatment.



Supplemental Figure 6

**Supplemental Figure 6.** *Postnatal analysis of Ryk conditional loss of function by*

*immunohistochemistry for MGE, CGE, and Oligodendrocyte markers. Related to figure 5.*

Representative examples of tdTomato<sup>+</sup> cells (red) in (A) P21 *Nkx2-1<sup>Cre</sup>; Ryk<sup>f/+</sup>* control and (B) *Nkx2-1<sup>Cre</sup>; Ryk<sup>f/f</sup>* mutant cortices scored for co-expression with somatostatin (SST, green) and parvalbumin (PV, blue). (A') Higher magnification of box in (A) *Ryk<sup>f/+</sup>* control cortex had few unidentified tdTomato<sup>+</sup> cells (denoted by asterisks) compared with (B) *Nkx2-1<sup>Cre</sup>; Ryk<sup>f/f</sup>* mutant. Pound sign denotes tdTomato/SST/PV triple-positive cell. tdTomato<sup>+</sup> cells (red) in (C) P21 *Nkx2-1<sup>Cre</sup>; Ryk<sup>f/+</sup>* control and (D) *Nkx2-1<sup>Cre</sup>; Ryk<sup>f/f</sup>* mutant cortex were scored for co-expression with Vasointestinal peptide (VIP, green) and Reelin (blue). TdTomato cells (red) in (E) P21 *Nkx2-1<sup>Cre</sup>; Ryk<sup>f/+</sup>* control and (F) *Nkx2-1<sup>Cre</sup>; Ryk<sup>f/f</sup>* mutant cortex stained for PEDGF (green) and Olig2 (white). Reporter labeled mutant cells do not adopt CGE or Oligo marker expression.